future internet

MDPI

Article

An Explainable Deep Learning-Enhanced IoMT Model for Effective Monitoring and Reduction of Maternal Mortality Risks

Sherine Nagy Saleh [1,*], Mazen Nabil Elagamy [1], Yasmine N. M. Saleh [2] and Radwa Ahmed Osman [3]

[1] Computer Engineering Department, College of Engineering and Technology, Arab Academy for Science and Technology (AAST), Alexandria 1029, Egypt; mazenelagamy@aast.edu
[2] Computer Science Department, College of Computing and Information Technology, Arab Academy for Science and Technology (AAST), Alexandria 1029, Egypt; yasmine_nagi@aast.edu
[3] Basic and Applied Science Department, College of Engineering and Technology, Arab Academy for Science and Technology (AAST), Alexandria 1029, Egypt; radwa.ahmed@aast.edu
* Correspondence: sherine_nagi@aast.edu

Abstract: Maternal mortality (MM) is considered one of the major worldwide concerns. Despite the advances of artificial intelligence (AI) in healthcare, the lack of transparency in AI models leads to reluctance to adopt them. Employing explainable artificial intelligence (XAI) thus helps improve the transparency and effectiveness of AI-driven healthcare solutions. Accordingly, this article proposes a complete framework integrating an Internet of Medical Things (IoMT) architecture with an XAI-based deep learning model. The IoMT system continuously monitors pregnant women's vital signs, while the XAI model analyzes the collected data to identify risk factors and generate actionable insights. Additionally, an efficient IoMT transmission model is developed to ensure reliable data transfer with the best-required system quality of service (QoS). Further analytics are performed on the data collected from different regions in a country to address high-risk cities. The experiments demonstrate the effectiveness of the proposed framework by achieving an accuracy of 80% for patients and 92.6% for regional risk prediction and providing interpretable explanations. The XAI-generated insights empower healthcare providers to make informed decisions and implement timely interventions. Furthermore, the IoMT transmission model ensures efficient and secure data transfer.

Keywords: explainable artificial intelligence; IoMT; maternal mortality; security and privacy; energy efficiency; machine learning

check for updates

Citation: Saleh, S.N.; Elagamy, M.N.; Saleh, Y.N.M.; Osman, R.A. An Explainable Deep Learning-Enhanced IoMT Model for Effective Monitoring and Reduction of Maternal Mortality Risks. *Future Internet* **2024**, *16*, 411. https://doi.org/10.3390/fi16110411

Academic Editor: Petros Patias

Received: 10 October 2024
Revised: 4 November 2024
Accepted: 6 November 2024
Published: 8 November 2024

Copyright: © 2024 by the authors. Licensee MDPI, Basel, Switzerland. This article is an open access article distributed under the terms and conditions of the Creative Commons Attribution (CC BY) license (https://creativecommons.org/licenses/by/4.0/).

1. Introduction

Undoubtedly, one of the problems facing the world is the morbidity and mortality of mothers because of pregnancy-related medical problems, which is still one of the major global challenges today. Every day, roughly 830 maternal fatalities worldwide result from problems during pregnancy or childbirth, and most of these phenomena could typically be avoided. By 2030, the Sustainable Development Goal 3 (SDG 3) of the United Nations seeks to increase maternal health and decrease the child and maternal mortality ratio (MMR) [1]. The MMR is a standardized method for calculating the number of women who die before, during, or within 42 days after giving birth to a child or while they are pregnant. The majority of these fatalities are caused by preventable factors, such as antepartum hemorrhage, postpartum hemorrhage, ruptured uterus, high blood pressure, severe bleeding, infection following pregnancy termination, and pulmonary embolism [2]. However, particularly in developing nations, the MMR has exceeded the predictions. Approximately 99% of maternal deaths from pregnancy and childbirth-related avoidable causes take place in underdeveloped nations [1,3,4].

Artificial intelligence (AI) has been expanded to several healthcare applications, including patient records and diagnosis, management of health services, and prognostic medicine. Despite performing at a level comparable to humans, AI models still have a limited range

of applications since their decisions are not always explainable. The limited adoption of AI in healthcare, particularly due to trust issues, can be addressed through explainable artificial intelligence (XAI). By providing clear explanations for model predictions, XAI can increase user confidence and promote the wider use of AI systems in healthcare [5].

In 2022, a survey was conducted by [6] to examine current research and development viewpoints that make use of AI techniques to forecast the ideal delivery mode and identify different difficulties during childbirth. Their review study analyzed the chosen AI algorithms and their performances, highlighted the goals of the most recent studies on pregnancy outcomes using AI, and gave a synthesized perspective of the features employed, types of features, data sources, and characteristics. The survey also outlined opportunities for future research to support current efforts to lower the MMR and complacency rates using unsupervised and deep learning algorithms for prediction, identifying the unidentified causes of maternal complications, creating practical and useful AI-based clinical decision support systems for use by expectant mothers and healthcare professionals, improving datasets and their accessibility, and investigating.

Accordingly, the contributions of this article can be summarized as follows:

- A proposed XAI region-based evaluation framework, in which an assessment of each region (city or state) to be determined defines whether or not it is classified as high or low risk.
- An XAI individual continuous monitoring scheme of pregnant women's vitals which issues an alert for medium- and high-risk cases. The focus on using an explainable model is an advantage in the proposed framework compared to previous research.
- A proposed deep learning model that is to be trained for the regions dataset, and then, analyzed. The same model structure but with an updated input and output size is trained for the patient dataset and analyzed.
- A proposed efficient and secure transmission of the data collected from pregnant women to the healthcare center.
- A performance assessment of the proposed deep learning model, including an XAI analysis of the results.

The rest of the article is organized as follows: first, the related work is presented. Afterwards, the proposed methodology for region-level and patient-level monitoring and efficient information transmission schemes is illustrated. The results are then reported and discussed. Finally, the conclusions and future work are presented.

2. Related Work

Several research articles have addressed the problem of the MMR. For instance, pregnant women in Afghanistan face several difficulties, including a shortage of medical centers, a lack of health information management systems in the majority of clinics and hospitals, a lack of doctors, cultural concerns, and issues with infrastructure and transportation, among others [7]. To address the issue of the MMR in Afghanistan, ref. [7] offered four proposals for using information communication technology (ICT), including the implementation of awareness campaigns through ICT, medical decision support systems, telemedicine, and healthcare information systems by applying different data mining (DM) and machine learning (ML) methods.

The Internet of Things (IoT) can be used in sectors that are vital to society like the healthcare sector [8,9]. Consequently, ref. [8] presented an efficient monitoring system for expectant mothers, primarily in remote areas of a poor country, with the aid of wearable sensing-enabled technology, notifying the expectant mother and her family about their health concerns.

In the same context, for efficient tracking and forecasting of a pregnant woman's risk level in Bangladesh, a collection of data on maternal health was assembled from various sources (IoT devices, web portals, and hospitals in Bangladesh) and saved on a cloud server by [9]. Their modified decision tree (DT) algorithm achieved a 97% accuracy in

predicting the risk level of pregnant women, which was the best compared to various ML classification techniques.

In 2021, ref. [10] conducted another MMR study in Bangladesh using bagging ensemble classifiers, a novel approach in the field of birth mode prediction built on some traditional ML algorithms. In their research, bagging ensemble classifiers were used to analyze the performance of four ML techniques (DT-Bagging, KNN-Bagging, NB-Bagging, and SVM-Bagging). The outcomes demonstrated that, in this area, bagging ensemble models outperformed conventional models. In the same context of studying the MMR in different countries, a nested ensemble system based on stacking and voting was proposed by [11] for the prediction and study of the MMR in India. By applying several classification algorithms, the provided nested ensemble includes base learners and meta-learners. The prediction results were then assessed using K-fold cross-validation, facilitating the statistical distribution of results. The experimental results of the study demonstrated that the best model for categorizing the maternal health data into high MMR and low MMR used random forest as the base learner in combination with two other base learners, logistic and PART, and two meta-learners, Hoeffding and REPTree.

Furthermore, ref. [12] used an electrocardiogram (ECG)-based DL model on a cohort of women examined at the Mayo Clinic who were pregnant or in the postpartum phase to diagnose cardiomyopathy, which is a significant risk to maternal health. The area under the receiver operating characteristic curve (AUC), along with accuracy, sensitivity, and specificity measures, was used to assess the performance of their model to compare it with natriuretic peptides and a multivariable model made up of clinical and demographic factors.

While these studies have made significant contributions to the field of maternal health, there is a growing need for interpretable and explainable AI models to improve trust and transparency in healthcare decision making. Article [13] has employed several machine learning models to classify the region-level risk. These models include logistic regression, classification and regression tree classifier, artificial neural networks, support vector machines, and random first. Their testing results showed that random forest and logistic regression had the best results. They also included an analysis of the selected models to show the explainability and importance of the features.

Article [14] conducted a survey on perinatal health predictors using AI, outlining and emphasizing the potential of AI-based algorithms and XAI techniques for the creation of novel prediction models, improved diagnosis, early detection, and monitoring of women during pregnancy, labor, and postpartum to advance research, clinical practice, and policies, and guarantee optimal perinatal health. According to article [15], model-specific or model-agnostic-based techniques are two broad categories under which XAI can be categorized. In general, many machine learning models, such as decision trees, rule-based models, and linear models, also referred to as transparent models or white-box models, are inherently interpretable. However, these straightforward models perform relatively worse than more complicated models. Model-specific and post hoc XAI algorithms could be created for each of the more complicated models, such as support vector machines (SVM), convolutional neural networks (CNNs), recurrent neural networks (RNNs), and ensemble models. For instance, frequently employed techniques include feature relevance explanation, architecture change, explanation by simplification, and explanation by visuals. In general, these more sophisticated models might perform better while losing explainability. It is important to emphasize that, given the nature of the issues, simpler models may still outperform deep learning-based models while maintaining explainability.

Table 1 summarizes the recent literature that addressed the maternal mortality problem. The table shows the datasets used for each study, the main methodology deployed, the best accuracy achieved, the region (city or state or country) in which the dataset was collected, and finally, the problem tackled by the research, addressing a monitoring technique to either predict maternal mortality risk or to predict region-level mortality. The table shows that most research achieves high results by using ensemble techniques, yet when the explainable AI approach was deployed, the results were much lower.

Table 1. Summary of recent literature addressing the problem of maternal mortality.

Ref.	Dataset	Methodology	Results (Acc)	Region	Problem Tackled
[9]	Collected by researchers	Modified decision tree-based technique	97%	Bangladesh	Monitoring of pregnant women
[10]	Collected by researchers	Bagging ensemble classifiers	87%	Bangladesh	Predicting type of birth
[11]	Health Management Information System	Nested ensemble	91.1%	India	Predicting region-level High/Low MMR
[16]	UCI repository	Multi-ensemble model	93.99%	Bangladesh	Predict mother risk level
[17]	Collected by researchers	Gradient boosting machine learning algorithm	90.24%	Ethiopia	Monitoring of pregnant women
[13]	Health Management Information System	Explainable AI	68%	India	Predicting region-level High/Low MMR

All the previous literature focused on addressing the MMR at the patient level by monitoring expectant mothers or at a country level by studying the risk factors. In this work, the MMR problem is addressed from a global perspective. The first scope is a country-based evaluation, in which an assessment of each city/state is made, defining whether or not it is classified as high or low risk. Since the city information is affected by the individual monitoring of the patients, the second scope is to continuously monitor pregnant women's vitals and issue an alert for medium- and high-risk cases. This information was efficiently and securely transmitted to the healthcare center and recorded in the patient's medical record, thus allowing intervention whenever needed. Since the topics addressed are very sensitive at the country level and the patient level, it became important to choose an explainable model that would provide an analytical evaluation of the results. Thus, in this work, models providing high performance like deep learning are compared to explainable models to help decide whether the performance degradation is acceptable as opposed to the model's interpretability.

3. Materials and Methods

As mentioned earlier, most research addresses the problem of the MMR through two separate perspectives: analyzing data at a regional or a patient level. The proposed model in this article comprises a complete framework for minimizing the MMR by presenting a framework that addresses both the region and patient levels with efficient transmission.

Furthermore, the presented framework's target is to employ deep learning models that can be used as explainable interfaces while maintaining performance, as the addressed problem is critical. Several learning models are tested to explore their performance versus the presented deep learning model.

3.1. Proposed Region-Level Monitoring Scheme

The idea behind region-level monitoring is to continuously gather information from different regions within a country and act accordingly. The collected data contain a comprehensive set of features capturing various aspects of maternal health, including demographic factors (population, number of pregnant women), healthcare access (antenatal care, skilled birth attendants), maternal health indicators (hypertension, anemia, complications), and birth outcomes (stillbirths, infant mortality). The proposed model analyzes these features to identify regions with high maternal mortality risk. The primary risk factors considered in this context include low levels of antenatal care, high rates of home deliveries, and poor maternal health indicators like anemia and hypertension.

To build this model, first, the information collected from the areas is assessed by experts and government personnel to determine which regions are considered to have a high mortality risk versus those that do not. The flagged data are then used to build an XAI model. Since the personnel discussing this problem are usually representatives from health institutions and the government, the outcome of the model needs to be not only the risk of the input region but also an explanation as to why it is marked as high risk such that the risk factors can be targeted independently. The proposed model is presented in Figure 1. The choice of the XAI is dependent on preserving the performance of the classification while maintaining the explainability of the model. This is further discussed and presented in the following section.

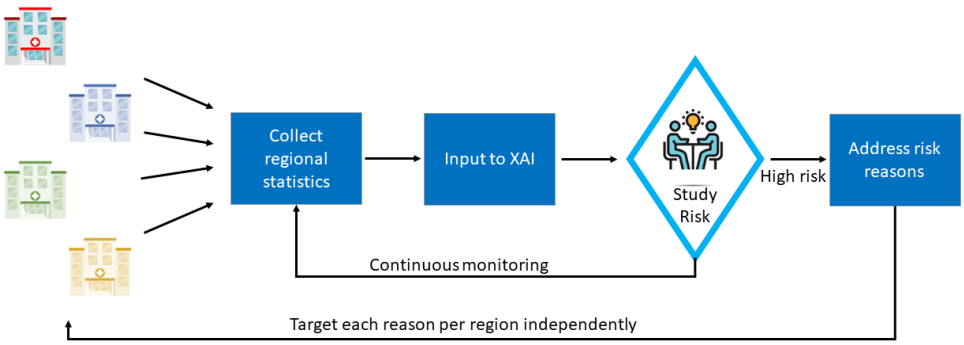

Figure 1. Proposed region monitoring scheme.

3.2. Proposed Patient Monitoring Scheme

In parallel to the region-level monitoring, there is a need to have a continuous basic monitoring scheme for women during and after pregnancy. Due to improper monitoring of maternal health during and after pregnancy, many women die from pregnancy-related illnesses. This is especially prevalent in rural and low-income urban areas of developing countries. Identifying the main causes of these maternal health issues is essential for implementing effective early warning systems [9]. Accordingly, the patient data focus on individual patient health metrics. They include physiological parameters such as blood pressure, blood sugar, body temperature, and heart rate, as well as demographic information like age and weight. These factors are very important when assessing a patient's risk of developing pregnancy-related complications. The proposed model analyzes these factors to identify the patients who are at high risk and provide timely interventions.

The Internet of Medical Things (IoMT) is a network of medical devices and applications that leverages IT to collect and transmit medical data for storage, analysis, and delivery of healthcare and e-healthcare services [18]. Following the basic architecture of the IoMT, the proposed model is presented in Figure 2, in which sensors (for example, those included in a health watch) are deployed to continuously collect readings to monitor the health condition of a pregnant woman. In this model, readings from blood pressure, pulse oximeter, temperature, and glucose level sensors are collected and input to a trained XAI model, which analyzes the data and accordingly produces the factors behind the risk, and accordingly, a physician may suggest a dietary or exercise recommendation to the patient. The collected sensor readings and the recommendation of the XAI model are collectively transmitted to a data center for storage, to the hospital, and/or to a physician responsible for the follow-up of the pregnant woman's state. Depending on her health condition, a hospital and/or a physician could remotely alter the medications of a pregnant woman and send back the new prescriptions, which could be automatically ordered through smart in-home devices.

Security and privacy are among the most critical challenges associated with the deployment of the IoMT. The IoMT includes various types of devices and connections that could be targets for security and privacy attacks resulting in the leakage of sensitive data and the possibility of data tampering causing inaccurate diagnoses, which in turn can

result in improper prescriptions, treatments, and in extreme cases could potentially be life threatening [18,19]. Recommendations for secure IoMT development fall into the following three categories: device security, connectivity security, and cloud security [20]. Possible security attacks on IoMT devices include side-channel attacks, device tampering, tag cloning, and sensor tracking. Attacks at the connectivity or network level include eavesdropping, replay, man-in-the-middle, rogue access, denial of service (DoS)/distributed denial of service (DDoS), sinkhole, sniffing, and selective forwarding. Finally, attacks at the cloud, data centers, or hospitals where data storage, analytics, and visualization are carried out include attacks such as brute force attacks, SQL injections, account hijacking, and ransomware [18]. To ensure the trust and confidence of IoMT stakeholders, various security measures should be implemented. To guarantee the legitimacy of participants and devices in the IoMT, diverse authentication schemes are deployed in the IoMT, such as key-based authentication, multi-factor authentication, and digital certificates [21,22]. In addition, encryption algorithms using public encryption keys such as Rivest–Shamir–Adleman (RSA) or elliptic-curve cryptography (ECC), or symmetric key algorithms such as Advanced Encryption Standard (AES) or Data Encryption Standard (DES), are crucial to ensuring secure data transmission and communication [22]. Furthermore, key management systems (KMSs) are used for the generation, distribution, and management of secret keys between the different communicating entities [23]. To illustrate a possible secure communication scenario, data collected from healthcare sensors, such as blood pressure or glucose level, are encrypted using an encryption protocol (AES-256, for example). The encrypted readings and the digital signatures of the sensors are securely transmitted over secure communication channels using the Transport Layer Security (TLS) protocol. At the recipient end, the digital signature is verified and the received data are decrypted [21].

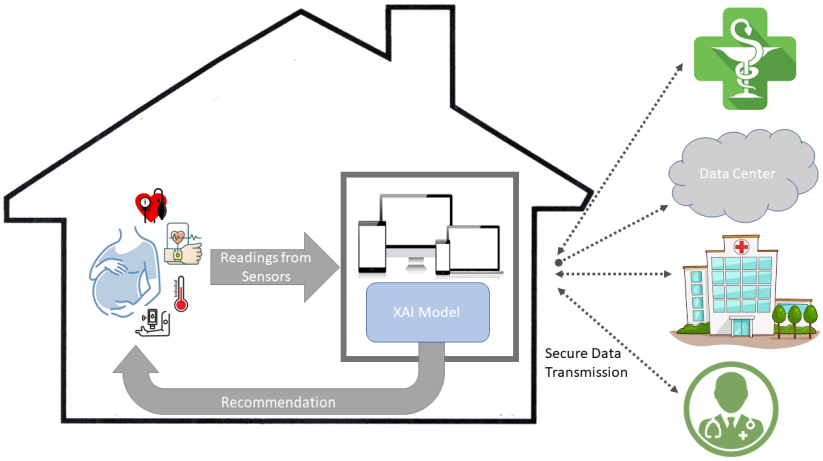

Figure 2. Proposed patient monitoring scheme.

With the high volumes of medical data being captured and sent over the IoMT, privacy is of paramount importance due to the presence of personal identifiable information (PII) [20]. Laws for data privacy and protection of medical data are enforced in countries to support fundamental privacy objectives like fairness, purpose fulfillment, proportionality, and accountability. Among these laws and initiatives are the Health Insurance Portability and Accountability Act (HIPAA), Health Information Technology for Economic and Clinical Health Act (HITECH), Personal Information Protection and Electronic Document Act (PIPEDA), and others [24]. Privacy protection mechanisms are applied in different aspects of the IoMT: data collection, data access, and data usage. Protection mechanisms for data collection include consent, opt-in, and fairness. Data access mechanisms dictate the pseudonymity (or anonymity) of the data owner, notification of when data are being collected, auditability (for controlled access to the data), and accountability. Finally, data usage privacy mechanisms should be guaranteed during the retention, disposal, and in

case of possible incidents or breaches in the handling of PII [20]. In this proposed model, the sensor readings collected from a pregnant woman and the XAI recommendations are encrypted and transmitted over a secure channel to the data centers, hospitals, and/or physicians. The pregnant woman's identity should remain anonymous on all records kept in the data centers and the hospital, as these records could be used later for further analysis to study the health conditions of a region.

3.3. Proposed XAI Deep Learning Model

The proposed XAI deep learning model, as presented in Figure 3, is a convolutional recurrent neural network (CRNN) that combines convolutional layers for feature extraction with gated recurrent units (GRUs) to capture temporal dependencies. Finally, a dense layer is added to perform classification. The final values of the model parameters are deduced by performing a grid search on different values for the filters, max pooling, inner dense layer shape, and dropout.

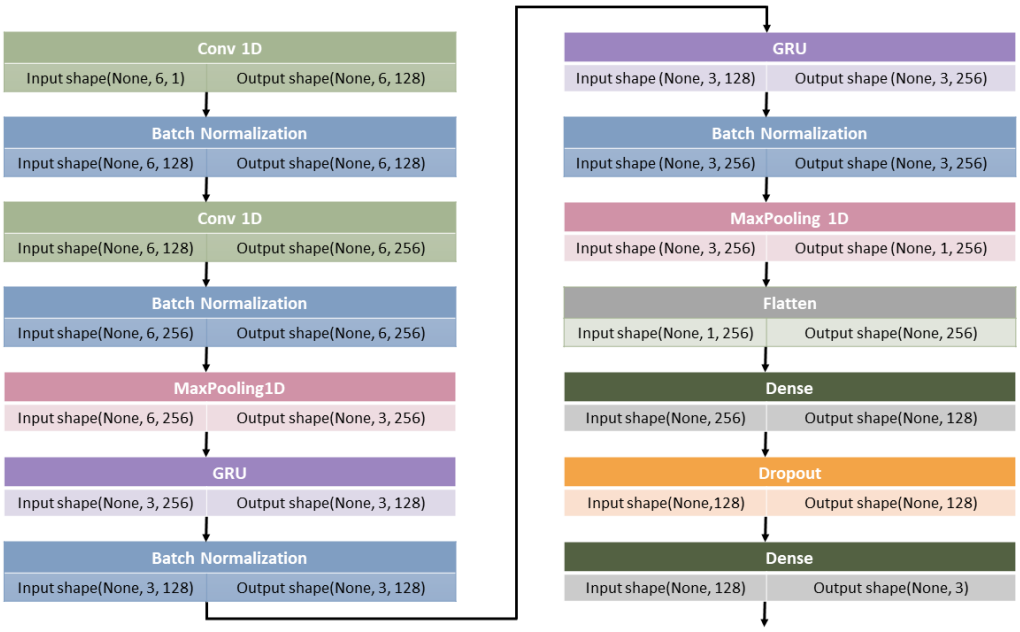

Figure 3. Proposed deep learning model for risk classification.

The model comprises convolutional layers to extract features from the input data using filters of size 3 and ReLU activation. Also, batch normalization layers are added to improve training stability. Following the CNN layers, GRU layers are added to further process the data and find more hidden patterns. The final layers represent the classification stage, where the data are flattened and dense layers with ReLU activation are employed with dropout to extract higher-level features and prevent overfitting.

The model is compiled using the Adam optimizer and categorical cross-entropy loss function, which is appropriate for multi-class classification tasks. Several metrics are monitored during training, including accuracy, precision, recall, area under the curve (AUC), and categorical accuracy. A checkpoint is used to save the best model based on the validation AUC. The presented model is interpreted through SHAP and LIME. It is to be noted that the input shape for the model is updated according to the number of features in the dataset and the output shape is dependent on the number of classes in the target feature.

3.4. Proposed Patient Information Transmission Scheme

The proposed framework utilizes an IoMT communication system to facilitate the transfer of patient data from various smart monitoring devices to a medical reception, as depicted in Figure 4. The presented framework aims to address the entire process of

collecting data from different sensors, applying XAI models for recommendations and analysis, and finally, securely and efficiently transmitting the data to remote locations for further analysis, storage, or request for intervention.

The proposed transmission scheme is an important part of this framework to ensure an optimized use of the wireless channels to achieve the lowest data loss during transmission with minimal energy consumption to produce the best possible quality of service (QoS). The IoMT transmission system consists of a patient's smart monitor device, which must access the wireless channel to effectively send the data through the gateway to the medical reception. The proposed IoMT transmission model is designed to efficiently transmit patient data, achieving the highest possible QoS to ensure that the transferred data are successfully received by the destination.

For achieving the required goals, an optimized energy-efficient model is proposed to enhance the system energy efficiency (EE) with the minimum required system outage probability (p_{out}) to ensure that the information is sent with the best QoS, i.e.,

$$Max \sum_{n=1}^{N} EE, \ \ s.t. \ \ C1 : Q_{UL} \geq 1 - p_{outUL}, \ \ s.t. \ \ C2 : Q_{DL} \geq 1 - p_{outDL} \tag{1}$$

where $C1$ and $C2$ represent the Lagrange multipliers for the optimization problem. $C1$ ensures that the uplink outage probability $p_{\text{out,UL}}$ meets the needed uplink QoS U_{UL}. $C2$ ensures that the downlink outage probability $p_{\text{out,DL}}$ meets the required downlink QoS U_{DL}.

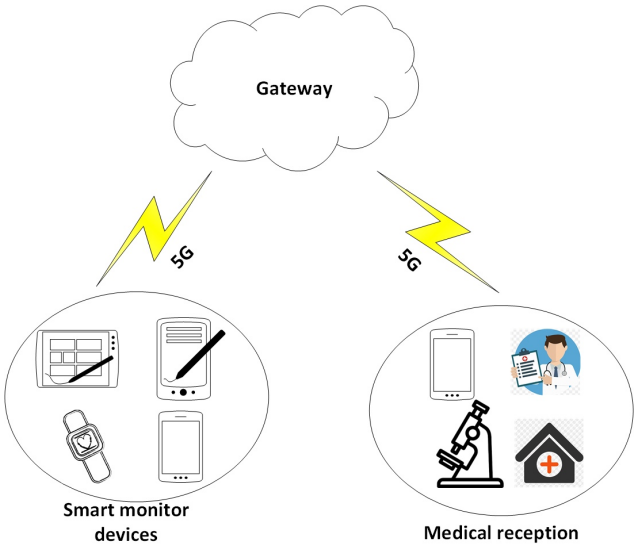

Figure 4. Proposed patient monitoring transmission scheme.

The link outage probability is defined as the probability that any receiver has a signal-to-interference plus noise ratio $(SINR)$ lower than the required threshold $(SINR_{th})$, let $(SINR_{th})$ be referred to as ξ. The required signal-to-interference plus noise ratio threshold for the uplink $(SINR_{thUL})$ and downlink $(SINR_{thDL})$ data transmission are referred to as ξ_{UL} and ξ_{DL}, respectively. Therefore, (p_{outUL}) and (p_{outDL}) can be formulated, respectively, as [25]

$$p_{outUL} = p(SINR_{thUL} \leq \xi_{UL}) = 1 - \frac{P_S|h_{SG}|^2}{\xi_{UL}\sum_{i=1}^{K} P_{IUi}|h_{IUiG}|^2 + P_S|h_{SG}|^2} e^{\frac{-\xi_{UL}N}{P_S|h_{SG}|^2}} \tag{2}$$

$$p_{outDL} = p(SINR_{thDL} \leq \xi_{DL}) = 1 - \frac{P_G|h_{GD}|^2}{\xi_{DL}\sum_{j=1}^{L} P_{IDj}|h_{IDjD}|^2 + P_G|h_{GD}|^2} e^{\frac{-\xi_{DL}N}{P_D|h_{GD}|^2}} \tag{3}$$

N denotes the noise power spectral density, expressed as $N = N_o B$, where B is the system bandwidth in hertz. Moreover, P_S and P_G represent the smart monitor device and the gateway

transmission power, respectively. The parameters $|h_{SG}|^2$ and $|h_{IUiG}|^2$ are the channel gain coefficients between the smart monitor device and the gateway and between any interfering devices and the gateway, respectively. Similarly, $|h_{GD}|^2$ and $|h_{IDjD}|^2$ represent the channel gain coefficients between the gateway and the medical reception, and between any interfering device and the medical reception, respectively. P_{IUi} and P_{IDj} denote the transmission powers of interfering devices to the gateway and the medical reception, respectively.

Assuming that $\xi_{UL}N \ll P_S|h_{SG}|^2$ and $\xi_{DL}N \ll P_G|h_{GD}|^2$, then Equations (2) and (3) can be rewritten as

$$p_{outUL} = p(SINR_{thUL} \leq \xi_{UL}) = 1 - \frac{P_S|h_{SG}|^2}{\xi_{UL}\sum_{i=1}^{K} P_{IUi}|h_{IUiG}|^2 + P_S|h_{SG}|^2} \tag{4}$$

$$p_{outDL} = p(SINR_{thDL} \leq \xi_{DL}) = 1 - \frac{P_G|h_{GD}|^2}{\xi_{DL}\sum_{j=1}^{L} P_{IDj}|h_{IDjD}|^2 + P_G|h_{GD}|^2} \tag{5}$$

$|h_{SG}|^2$, $|h_{IUiG}|^2$, $|h_{GD}|^2$, and $|h_{IDjD}|^2$ can be expressed as [26]

$$|h_{SG}|^2 = \frac{|h_{oSG}|^2}{PL_{SG}} \tag{6}$$

$$|h_{IUiG}|^2 = \frac{|h_{oIUiG}|^2}{PL_{IUiG}} \tag{7}$$

$$|h_{GD}|^2 = \frac{|h_{oGD}|^2}{PL_{GD}} \tag{8}$$

$$|h_{IDi} = j_D|^2 = \frac{|h_{oIDjD}|^2}{PL_{IDiD}} \tag{9}$$

where $|h_{oSG}|^2$, $|h_{oIUiG}|^2$, $|h_{oGD}|^2$, and $|h_{oIDiD}|^2$ follow a complex normal distribution $CN \sim (0, 1)$. The parameters PL_{SG}, PL_{IUiG}, PL_{GD}, and PL_{IDiD} represent the signal attenuation between the smart monitor device and the gateway, between interfering devices and the gateway, between the gateway and the medical reception, and between interfering devices and the medical reception, respectively.

Additionally, Rayleigh fading channels with additive white Gaussian noise (AWGN) [25] were assumed for both uplink and downlink transmissions. Non-orthogonal multiple access (NOMA) [27,28] was considered as the multiple access scheme. Furthermore, it was assumed that the channel fading coefficients for uplink and downlink transmissions were statistically independent. Thus, the overall system energy (EE) is expressed as

$$EE = \frac{B\log_2(1 + SINR_{thUL})}{P_S + P_o} + \frac{B\log_2(1 + SINR_{thDL})}{P_G + P_o} \tag{10}$$

$$SINR_{thUL} = \frac{P_S|h_{SG}|^2}{\sum_{i=1}^{K} P_{IUi}|h_{IUiG}|^2 + N} \tag{11}$$

$$SINR_{thDL} = \frac{P_G|h_{GD}|^2}{\sum_{j=1}^{L} P_{IDj}|h_{IDjD}|^2 + N} \tag{12}$$

where P_o represents the internal circuitry power. The optimization problem in Equation (1) can be solved using the first-order optimal conditions. Hence, the Lagrange optimization problem can be formulated as follows:

$$L(EE, \lambda_1, \lambda_2) = EE + \lambda_1(Q_{UL} - 1 + p_{outUL}) + \lambda_2(Q_{DL} - 1 + p_{outDL}) \tag{13}$$

where λ_1 λ_2 are non-negative values associated with constraints C1 and C2, respectively. By taking the derivative of Equation (13) with respect to P_S and P_G, the optimal solution of Equation (1) can be obtained as follows:

$$\frac{\partial L(EE, \lambda_1, \lambda_2)}{\partial P_S} = 0 \tag{14}$$

$$\lambda_1 = X_1 * B * (X_2 - X_3) \tag{15}$$

where $X_1 = (\frac{(\xi_{UL} \sum_{i=1}^{K} P_{IUi}|h_{IUiG}|^2 + P_S|h_{SG}|^2)^2}{\xi_{UL} \sum_{i=1}^{K} P_{IUi}|h_{IUiG}|^2})$, $X_2 = (\frac{|h_{SG}|^2}{(P_S+P_o)(1+\xi_{UL})(\sum_{i=1}^{K} P_{IUi}|h_{IUiG}|^2+N)})$, and $X_3 = (\frac{B \log_2(1+\frac{P_S|h_{SG}|^2}{\sum_{i=1}^{K} P_{IUi}|h_{IUiG}|^2+N})}{(P_S+P_o)^2})$.

$$\frac{\partial L(EE, \lambda_1, \lambda_2)}{\partial P_G} = 0 \tag{16}$$

$$\lambda_2 = X_4 * B * (X_5 - X_6) \tag{17}$$

where $X_4 = (\frac{(\xi_{DL} \sum_{j=1}^{K} P_{IDj}|h_{IDjD}|^2 + P_G|h_{GD}|^2)^2}{\xi_{DL} \sum_{j=1}^{L} P_{IDj}|h_{IDjG}|^2})$, $X_5 = (\frac{|h_{GD}|^2}{(P_G+P_o)(1+\xi_{DL})(\sum_{j=1}^{L} P_{IDj}|h_{IDjD}|^2+N)})$, and $X_6 = (\frac{B \log_2(1+\frac{P_G|h_{GD}|^2}{\sum_{j=1}^{L} P_{IDj}|h_{IDjD}|^2+N})}{(P_G+P_o)^2})$. Consequently, when considering the derivation of Equation (13) with respect to λ_1 and λ_2, respectively, it can be found that

$$\frac{\partial L(EE, \lambda_1, \lambda_2)}{\partial \lambda_1} = 0 \tag{18}$$

$$\frac{\partial L(EE, \lambda_1, \lambda_2)}{\partial \lambda_2} = 0 \tag{19}$$

therefore, based on Equation (18) and Equation (19) the required smart monitor device and gateway transmission can be expressed, respectively, as

$$P_{Sreq} = \frac{Q_{UL}\xi_{UL} \sum_{i=1}^{K} P_{IUi}|h_{IUiG}|^2}{(1 - Q_{UL})|h_{SG}|^2} \tag{20}$$

$$P_{Greq} = \frac{Q_{DL}\xi_{DL} \sum_{j=1}^{L} P_{IDj}|h_{IDjD}|^2}{(1 - Q_{DL})|h_{GD}|^2} \tag{21}$$

3.5. Datasets

To help test the proposed idea through an XAI interface, two different datasets were deployed, each conveying part of the required concepts. The first represented a region-level dataset and the other represented basic patient-level data collected from sensors.

3.5.1. Region-Level Dataset

The Government of India has implemented several schemes for improving the health of pregnant women of reproductive age, particularly addressing the challenges posed by early marriage, poverty, unsafe abortions, and short birth intervals, especially for women in remote areas. The Health Management Information System portal of the Ministry of Health and Family Welfare was the source of the first dataset (first presented in [11]) needed for this study, which included 33 metrics and data for all 674 of India's districts. Out of 674 districts, 386 showed a high MMR, while the remaining 288 were determined to have a low MMR. Additionally, the class label for the current work was a flag variable called MMR with the values high and low representing the risk of mortality. The parameters of the region-based MMR assessment dataset along with statistical analysis of each feature showing the mean, standard deviation (std), minimum (min), maximum (max), and the interquartile values (25%, 50%, and 75%) are presented in Table 2.

Table 2. The parameters of the region-based MMR assessment dataset.

Feature Name	Description	Mean	Std	Min	0.25	0.50	0.75	Max
POPULATION	Total number of people in the analyzed area	1,825,484.00	1,563,891.00	7948.00	738,538.50	1,485,979.50	2,530,096.50	12,478,447.00
T_PW_ANC	Total number of pregnant mothers who have signed up for antenatal care	42,229.54	37,032.84	172.00	16,120.25	32,908.00	57,284.00	240,798.00
T_PW_1TRI	Number of first-trimester registrations for prenatal care out of the total	26,508.65	21,734.53	93.00	11,545.75	22,015.00	35,869.50	144,797.00
PW_3ANC	Count of pregnant women who have had four or more prenatal care visits	31,717.64	27,085.62	55.00	13,251.25	25,965.50	44,096.50	227,511.00
PW_TT1	Count of pregnant women who have had tetanus toxoid 1 vaccination	31,549.00	27,372.80	97.00	13,185.75	24,542.50	42,237.00	177,174.00
PW_TT2	Count of pregnant women who have had tetanus toxoid 2 vaccination	35,044.82	29,650.66	94.00	14,389.25	28,744.50	48,060.00	187,706.00
PW_100IF:A	Count of pregnant women who have had 180 folic acid tablets	33,771.96	32,711.85	119.00	12,620.50	25,079.50	45,767.50	272,025.00
N_PW_HYP	Count of newly pregnant women suffering from hypertension	1328.42	1827.28	0.00	258.25	673.00	1665.00	16,502.00
N_ECL_D	Count of cases of eclampsia handled during delivery	92.37	198.60	0.00	9.25	41.00	101.50	2650.00
N_PW_HB11	Count of pregnant women with hemoglobin levels under 11 and greater than 7	24,146.60	23,422.15	5.00	8374.00	18,719.00	32,348.25	154,085.00
N_PW_HB7	Count of pregnant women with hemoglobin levels under 7	727.89	966.06	0.00	109.75	380.50	983.75	10,565.00
N_HD_SBA	Count of home deliveries performed by a skilled birth attendant	738.76	1467.64	0.00	30.00	174.00	750.00	15,130.00
N_HD_NSBA	Count of home deliveries performed by a non-skilled birth attendant	2450.95	4620.54	0.00	71.50	583.00	2552.50	27,019.00
T_HD_TNSBA	Count of home deliveries performed by trained or non-trained skilled birth attendant	3190.09	5579.94	0.00	173.25	916.50	3514.25	33,199.00
D_PI_C	Count of institutional deliveries, including c-section	21,757.52	17,491.30	65.00	9133.25	18,678.00	30,122.00	113,830.00
N_DIS_48H	Number of women dismissed from an institution after 48 h	9511.52	11,732.30	0.00	1423.75	5058.00	13,065.25	77,957.00
T_CS_PF	Total count of c-sections performed	2944.04	4362.10	0.00	342.75	1363.50	3648.25	39,204.00
N_MLB	Count of live male babies	16,015.47	13,170.06	35.00	6348.75	13,259.00	22,242.00	81,589.00
N_FLB	Count of live female babies	14,800.31	12,128.58	36.00	5864.75	12,219.00	20,992.50	76,230.00
T_MFLB	Total count of live male and female babies	30,816.13	25,291.94	71.00	12,237.75	25,601.50	43,320.00	157,820.00
N_SB	Count of lost pregnancies (stillbirth)	440.16	404.10	1.00	146.25	344.50	625.50	2891.00
N_ABO	Count of abortions	1244.03	2111.67	0.00	294.00	707.00	1464.75	30,295.00
N_NBW_B	Count of newborns assessed at birth	28,995.15	23,393.00	64.00	11,923.50	24,232.50	40,303.25	146,294.00
N_NBW_2.5	Count of newborns weighing less than 2.5 kg	3557.84	3481.62	1.00	1263.25	2794.50	4853.75	28,749.00
N_NB_BF_1	Count of newborns breast-fed within an hour of birth	27,329.86	22,197.45	64.00	10,712.00	22,701.50	39,017.25	132,783.00
N_PW_OC_PF	Count of cases with obstetric complications	2566.09	3455.36	0.00	502.50	1382.50	3264.25	28,334.00
N_CP_BT	Count of complicated cases treated with blood transfusion	697.85	1044.13	0.00	86.25	333.50	879.25	7973.00
W_PP_48H	Count of women receiving postpartum care within 48 h in case of home delivery	17,947.94	14,419.61	61.00	7192.00	15,851.50	24,804.25	105,923.00
W_PP_14D	Count of women receiving postpartum care between 48 h and 14 days post-delivery	17,244.65	15,325.15	28.00	6942.00	14,063.50	23,010.50	116,433.00
MTP_PI_12W	Count of medical terminations of pregnancy up to 12 weeks	623.64	1346.31	0.00	85.00	278.50	694.75	26,028.00
MTP_PI_M12W	Count of medical terminations of pregnancy after 12 weeks	71.14	218.98	0.00	3.00	18.00	66.00	3810.00
T_MTP_PI	Total count of medical terminations of pregnancy	695.12	1459.35	0.00	100.25	311.00	772.50	27,667.00
MMR	Maternal mortality ratio, classified as low or high	0.57	0.50	0.00	0.00	1.00	1.00	1.00

3.5.2. Patient Dataset

In low-income nations like Bangladesh, maternal mortality is increasingly a worrying aspect. In [9], an IoT-based maternal health care system was proposed to address this problem. Analyzing medical profiles, including age, weight, blood pressure, pre-existing conditions, heart rate, body temperature, and physical activity, allows for the prediction of risk levels for a certain patient based on these characteristics and their associated values. The research studied the symptoms as well as maternal health risk factors and collected data accordingly. The dataset comprises the most common readings that need to be monitored regularly from home via sensors. The readings of systolic blood pressure (SystolicBP), diastolic blood pressure (DiastolicBP), blood sugar level (BS), body temperature (BodyTemp), and heart rate (HeartRate) were reported along with the risk-level factor, categorized as low, mid, or high. This dataset is employed to mimic the patient-level monitoring presented in this research. The parameters of the dataset are shown in Table 3 along with a statistical analysis of each feature.

Table 3. The parameters of the patient-based MMR assessment dataset.

Feature Name	Description	Mean	Std	Min	0.25	0.50	0.75	Max
Age	Patient age	29.87	13.47	10.00	19.00	26.00	39.00	70.00
SystolicBP	Systolic blood pressure	113.20	18.40	70.00	100.00	120.00	120.00	160.00
DiastolicBP	Diastolic blood pressure	76.46	13.89	49.00	65.00	80.00	90.00	100.00
BS	Blood sugar level	8.73	3.29	6.00	6.90	7.50	8.00	19.00
BodyTemp	Body temperature	98.67	1.37	98.00	98.00	98.00	98.00	103.00
HeartRate	Heart rate	74.30	8.09	7.00	70.00	76.00	80.00	90.00
RiskLevel	MMR risk level	0.87	0.81	0.00	0.00	1.00	2.00	2.00

3.6. Assessment Methods

To best evaluate the machine learning methods used, the following metrics are used:

- Accuracy: The percentage of correctly classified samples over the total count of samples.
- Precision: The ratio of true positives to the total number of positives predicted by a model.
- Recall: The ratio of the true positives to the actual positives available.
- F-measure: The harmonic mean of the model's precision and recall is known as the F-score, which is a method of combining the model's precision and recall.
- AUC: Represents the area beneath the curve plot between the TP and FP rates.

Also, a further evaluation step is performed to assess the feature's importance. After the model assessment phase, the influence of the different features on the results is then evaluated using SHAP and LIME.

4. Results

This article aims to propose two XAI-based models for use in monitoring the MMR risk in a certain region in a country and at the patient level by ensuring that the patient's information is sent to the medical reception through an efficient communication system. The following subsections represent the experiments and the results for each part.

Region-level data results:

To propose an XAI model, extensive assessment of the available features is required, as this helps understand the relationships among the features and their effect on the results. The parameters of the region-level dataset were first analyzed by checking the Pearson correlation of the 33 parameters, as shown in Figure 5. The figure shows that all the features have a low-to-average correlation with the class MMR. There is a high correlation between

some of the features and others, which helps physicians better understand the relations among the different factors.

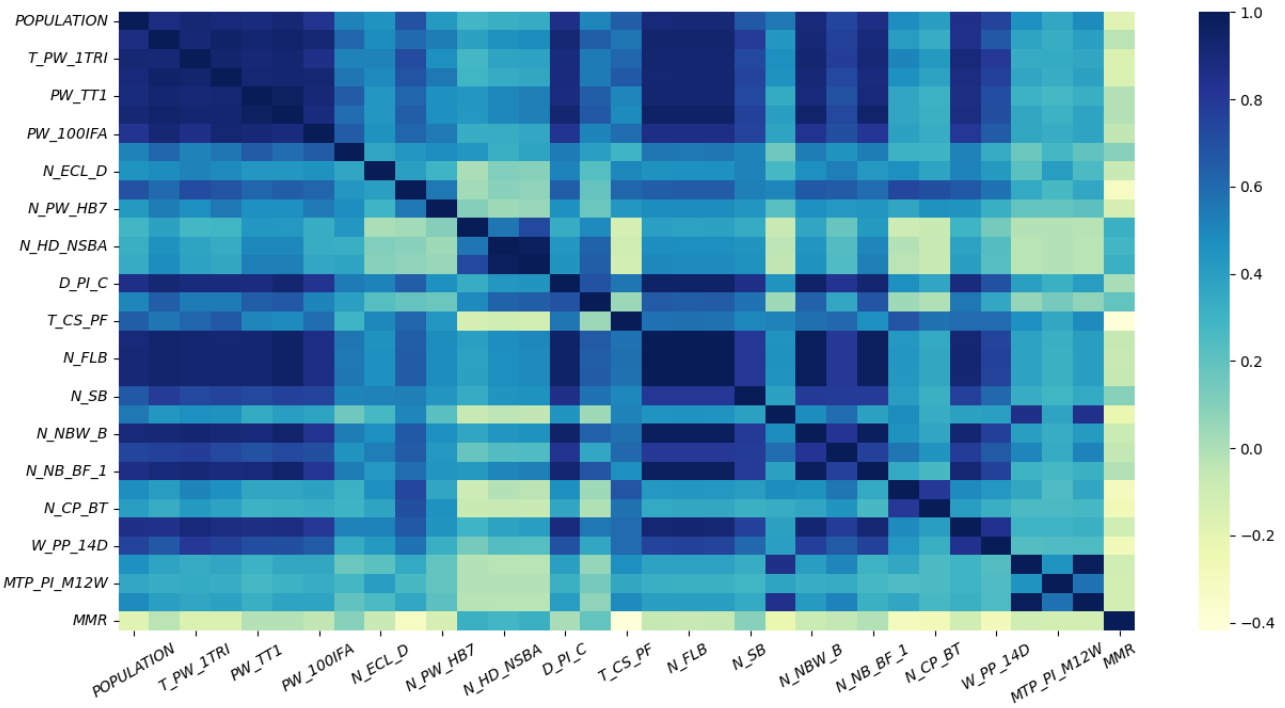

Figure 5. Pearson correlation of the region-based MMR assessment using all 33 features. The naming labels denote only the odd features from the list.

To evaluate the performance of different models in classifying state risk, several experiments were conducted using the entire dataset and 10-fold cross-validation. A variety of machine learning methods were employed, like decision tree (DT), logistic regression (LR), support vector classifier (SVC), and multi-layer perceptron (MLP) versus the proposed CNN-GRU model. The DT model employed the Gini index according to the best split. The LR model used was the default, which attempts to calculate an intercept term. The SVC model uses the radial basis function (RBF) kernel and a regularization parameter C of 1.0. The results, summarized in Table 4, demonstrate the superiority of the proposed CNN-GRU deep learning model. The MLP has a single hidden layer with 100 neurons, employing the ReLU activation function, and is trained with the Adam optimizer. It consistently achieves higher accuracy, precision, recall, F1-score, and AUC compared to all the other models considered.

Table 4. Different assessment results for various models on the region dataset.

	Accuracy	**Precision**	**Recall**	**F1-Score**	**AUC**
DT	0.857	0.858	0.857	0.857	0.970
LR	0.896	0.899	0.896	0.896	0.969
SVC	0.881	0.884	0.881	0.880	0.967
MLP	0.815	0.844	0.815	0.812	0.969
Proposed	0.926	0.926	0.926	0.926	0.970

The proposed model was trained for 200 epochs, as shown in Figure 6. By analyzing the charts it can be noted that there was no further improvement expected after epoch 200 and the shape of the curves suggests that the presented model did not overfit using the data at hand.

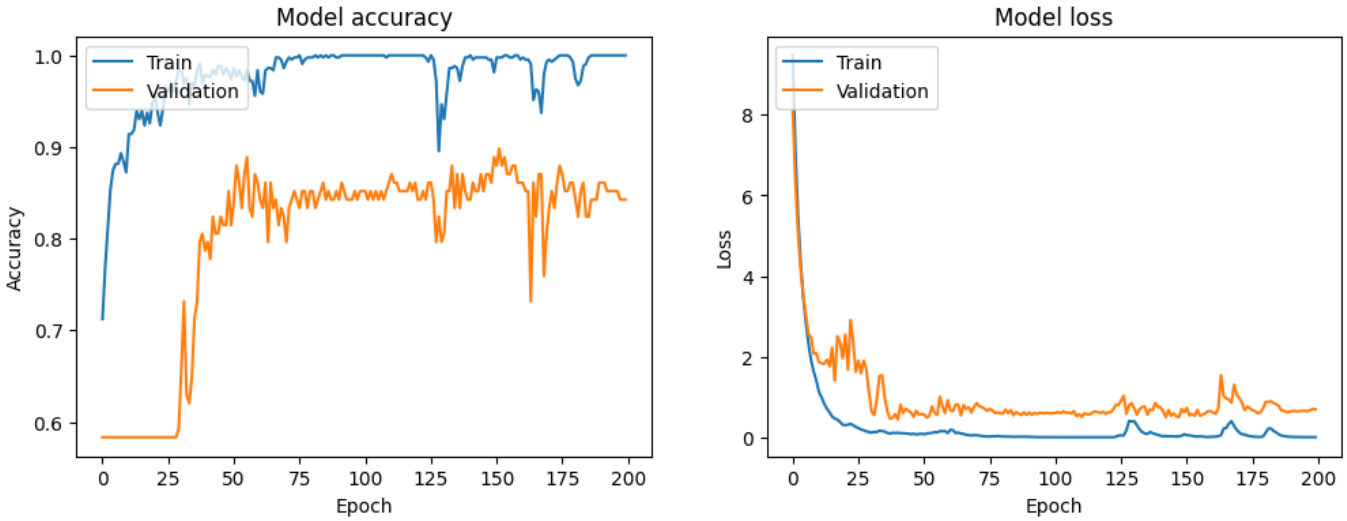

Figure 6. Accuracy and loss training and validation charts for the state dataset.

Figure 7 shows the SHAP summary for the two classes addressed in the region dataset. The feature influence on the low-risk class is shown in Figure 7a and the high-risk in Figure 7b. For instance, high features N_DIS_48H, T_HD_TNSBA, and N_NB_BF_1 negatively influence the low-level risk and vice versa for the high-level risk. According to Figure 7b, it can be deduced that several factors affect the high mortality risk; for example, an increase in the number of women dismissed from an institution after 48 h in a certain region (N_DIS_48H), an increased count of home deliveries (T_HD_TNSBA), an increased count of newborns breast-fed within an hour of birth (N_NB_BF_1), a low count of institutional deliveries, including c-section (D_PI_C), and an increased count of pregnant women with hemoglobin levels between 7 and 11 (N_PW_HB11). Accordingly, such factors could be addressed within a region to reduce the mortality risk.

Furthermore, the results of the proposed model can be compared with those achieved by [13], as they used the same dataset. The proposed explainable model produced 24% higher testing accuracy than their explainable approach. Also, the results exceeded those achieved by article [11], which presented an ensemble non-explainable model, by about 1.5%.

4.1. Patient Data Results

The Pearson correlation of the dataset is presented in Figure 8. It can be noted that the risk level has a higher correlation with blood sugar and blood pressure than the other features. All features have a low-to-medium correlation with the RiskLevel class. The number of available features and the correlation plot show that there is no need for feature selection in this part of the work.

Further analysis of the available features is presented in Figure 9. The plot shows the range of values for each feature and the existence of any outliers from the most common values. Since this is an XAI system, different data representations are required for medical personnel to monitor and understand the various factors affecting the patient's risk.

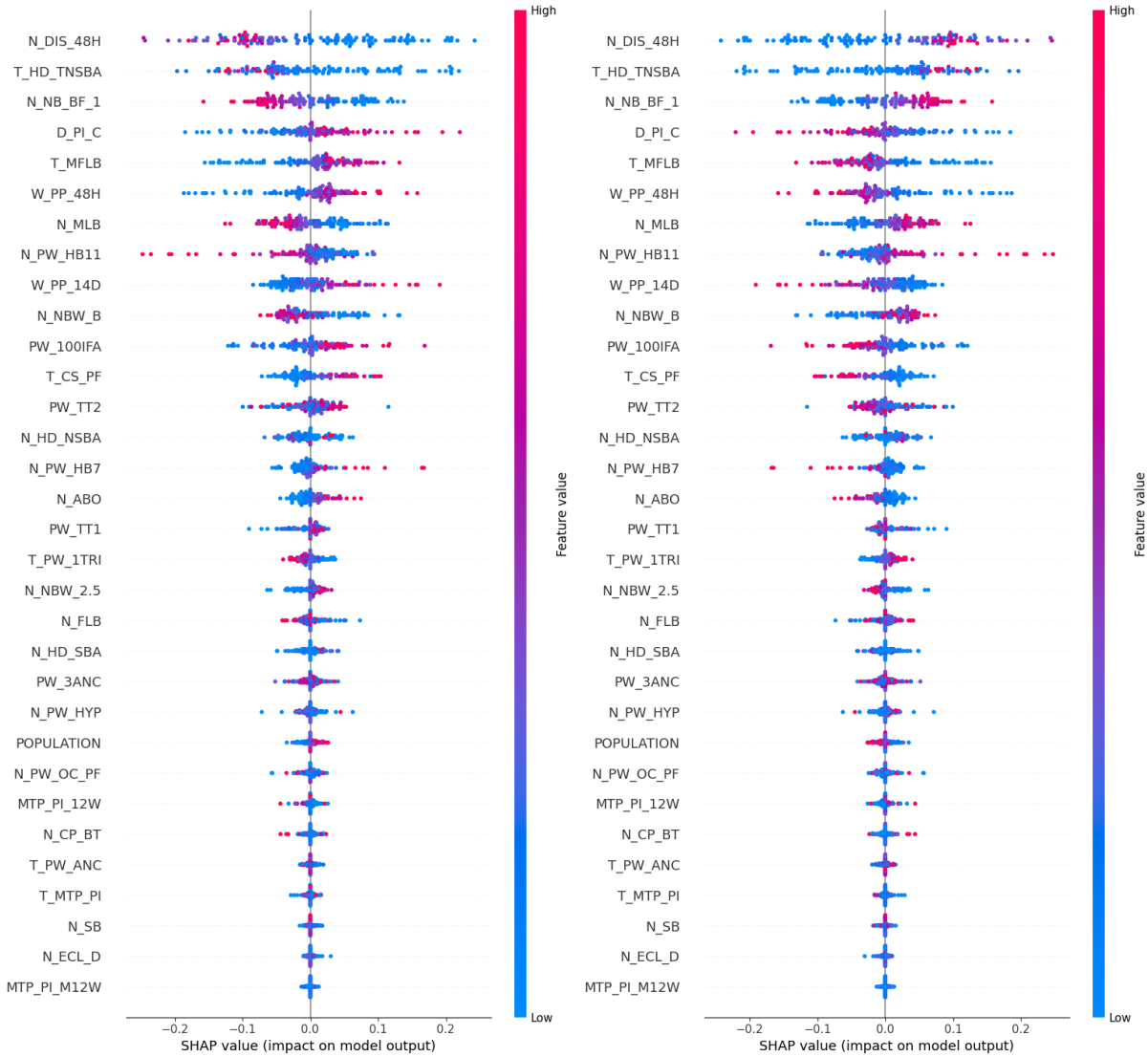

Figure 7. Feature influence on the low-risk class (**a**) and the high-risk class (**b**) in the region dataset.

The influence of each feature on the different risk levels is represented in Figure 10. It can be noted from the figure that high values of BS and BodyTemp can help identify low-risk versus high-risk patients but are less powerful in the mid-risk class. To further explore the aspect of explainability, three patient samples were analyzed using the LIME model, as represented in Figure 11. The three subfigures show a patient at low risk (Figure 11a), another at a mid-level of risk (Figure 11b), and one at high risk (Figure 11c). The low-risk patient analysis shows that the BodyTemp and BS were the most influential factors, resulting in a probability of 0.57 for this patient as a low-risk patient versus 0.22 and 0.21 for mid- and high-risk, respectively. In Figure 11b, the patient represented with a BS value of 9 was classified as mid-risk mainly because of this feature, with a probability of 0.41. Finally, the patient record represented in Figure 11c was classified by the model as high risk with a probability of 0.58 because of the values of the features SystolicBP, BS, and BodyTemp.

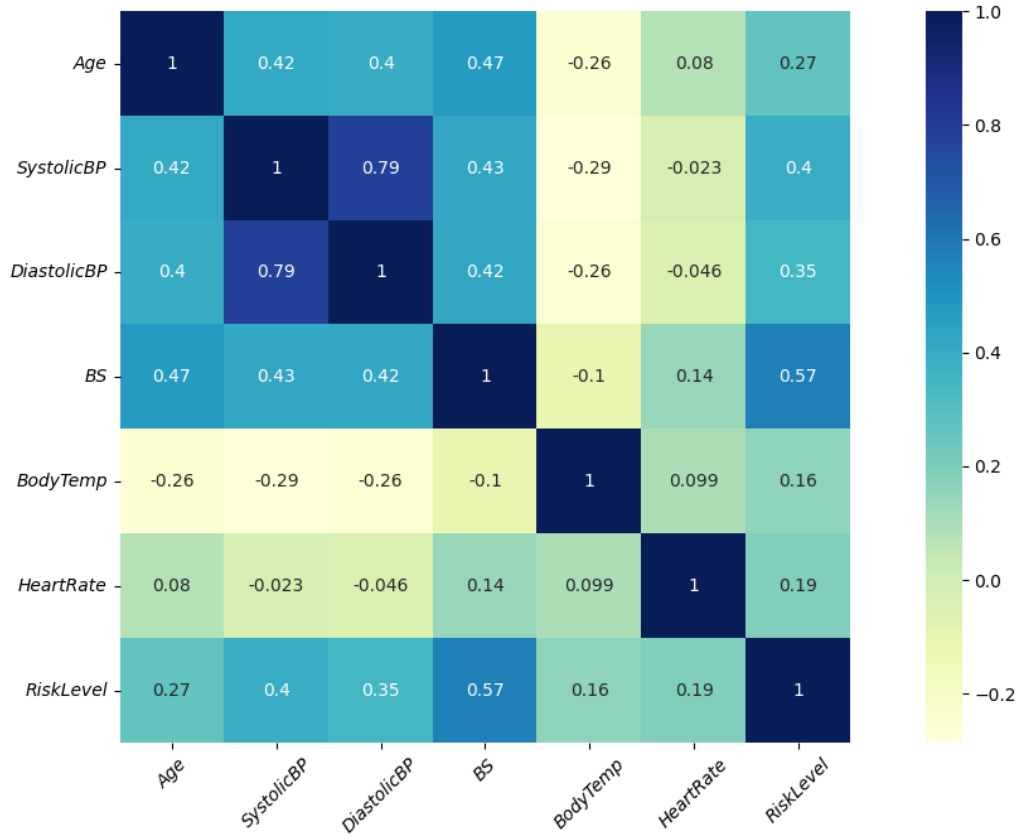

Figure 8. Pearson correlation of the dataset features.

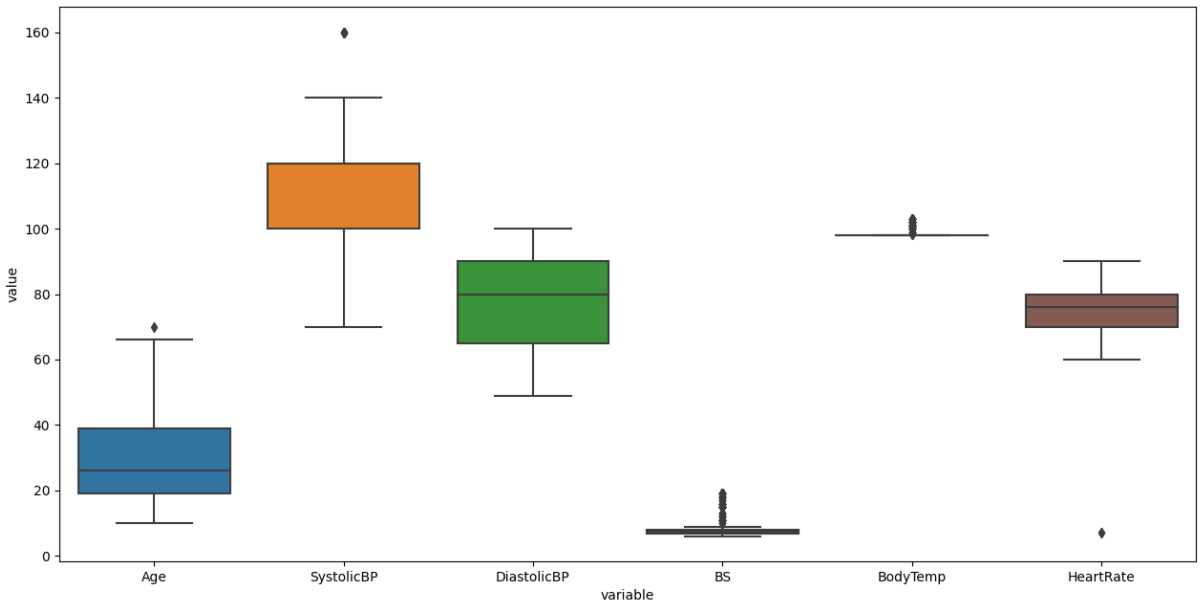

Figure 9. Box plot showing the range of values for each feature and whether there are any outliers.

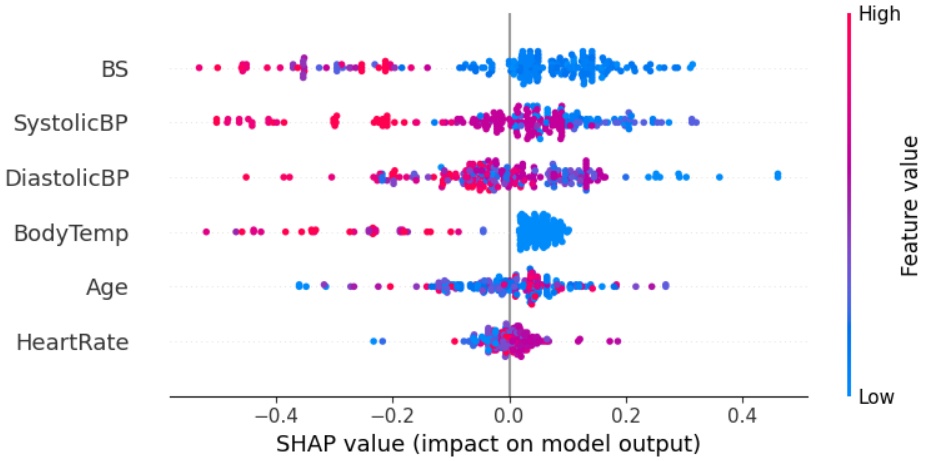

(**a**)

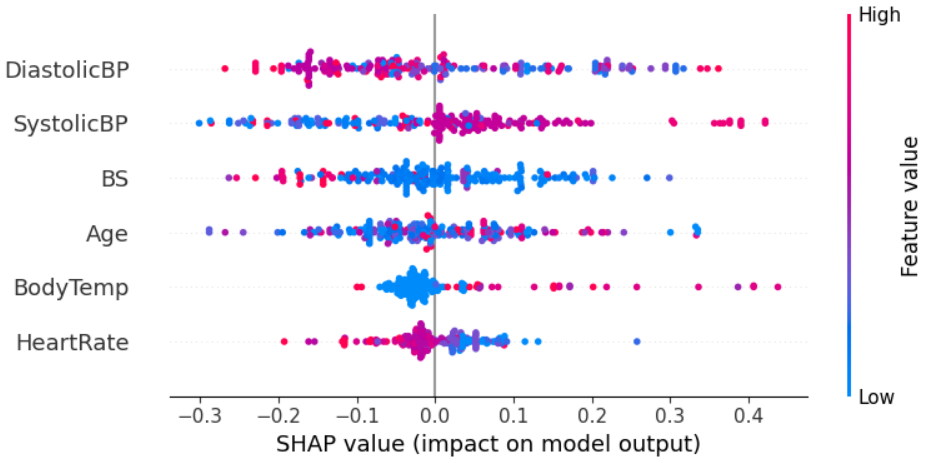

(**b**)

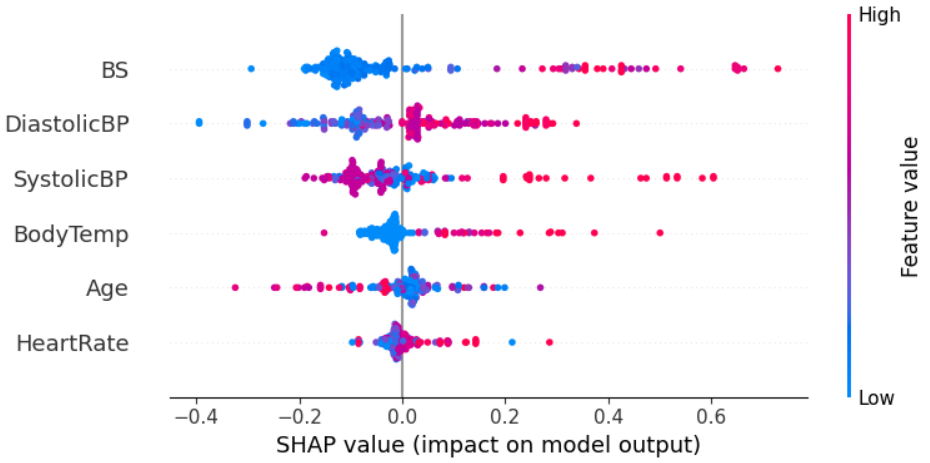

(**c**)

Figure 10. SHAP summary showing feature influence for low-risk (**a**), medium-risk (**b**), and high-risk (**c**) patients.

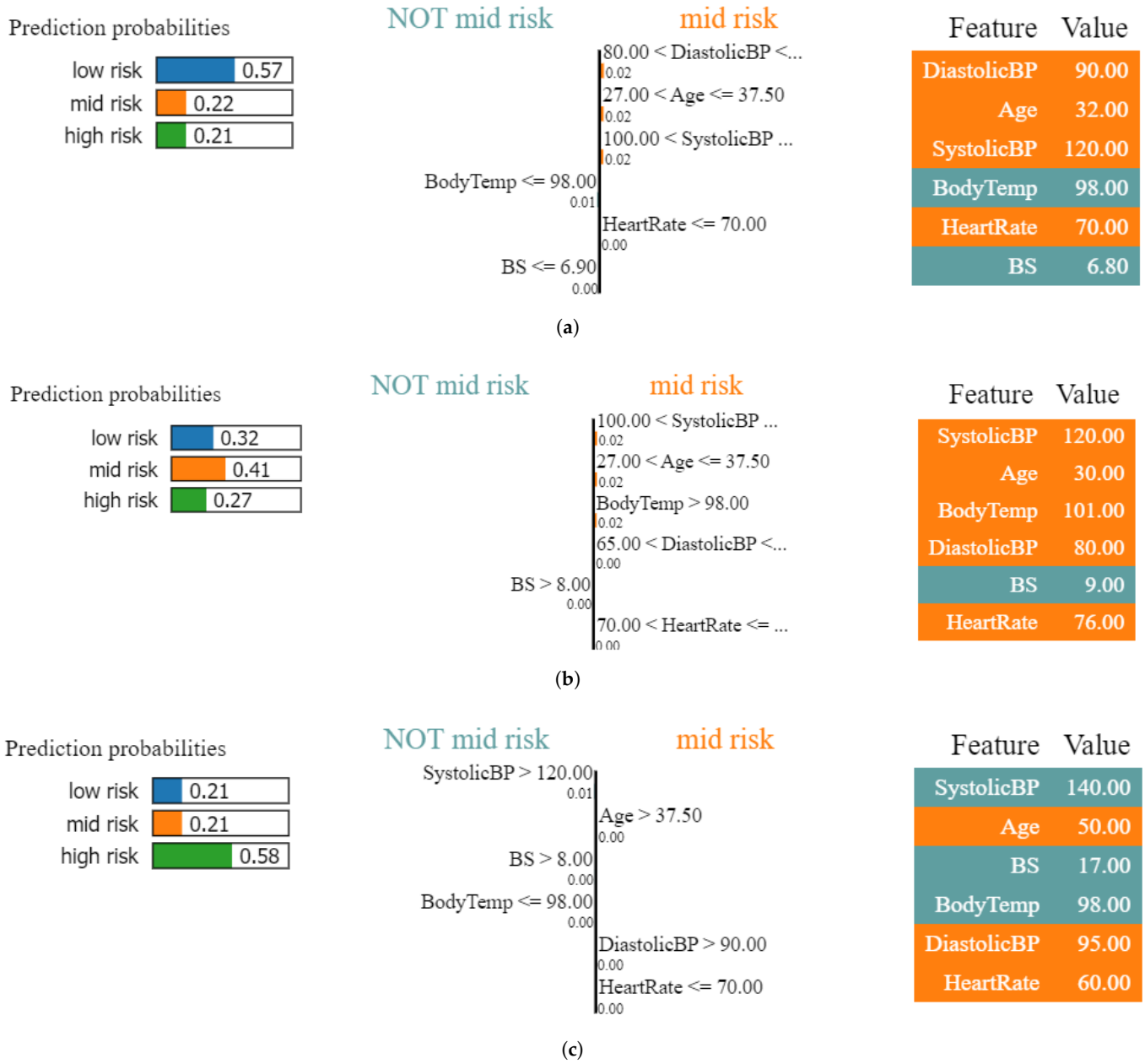

Figure 11. LIME analysis for three different patient records: one at low risk (**a**), another at a mid-level of risk (**b**), and the final at high risk (**c**).

The data were used in a 10-fold cross-validation manner to test multiple classifiers, as shown in Table 5. Similar to the region-level monitoring, different models were used to compare their performance versus the proposed model. The best results were achieved by the proposed CNN-GRU model in terms of accuracy, precision, recall, F1-score, and AUC. This suggests that the proposed CNN-GRU model is well suited for this task as well, effectively identifying dependencies in the patient data.

Table 5. Different assessment results for various models on the patient dataset.

	Accuracy	Precision	Recall	F1-Score	AUC
DT	0.777	0.781	0.777	0.776	0.821
LR	0.650	0.659	0.650	0.612	0.816
SVC	0.655	0.68	0.655	0.622	0.812
MLP	0.680	0.690	0.680	0.670	0.877
Proposed	0.803	0.803	0.803	0.803	0.912

4.2. Analytical Results

In this subsection, the simulation of the proposed analytical problem illustrated in Section 3.4 is simulated using MATLAB. The parameters implemented in the simulation are stated in Table 6. Figure 12 shows the required smart monitoring device transmission power P_{Sreq} and the required gateway transmission power P_{Greq} with different values of interfering device transmission power. From Figure 12, it can be observed that the required transmission power during the uplink and downlink data transmission to achieve the best system QoS must increase when the interfering device transmission power increases. This is because increasing the interference power affects the received data and causes loss of information, which will be critical in some pregnant women's cases. Thus, increasing the transmission power during the uplink and downlink data transmission leads to overcoming the interference, thus helping the information reach the destination most efficiently and accurately.

Table 6. Simulation parameters.

Parameter	Value
N_o	-174 dB/m [29]
B	10 MHz [30]
ξ_{UL} and ξ_{DL}	20 dB [31]
PL_{SG}	$128.1 + 37.6log_{10}(d_{SG})$ [32]
PL_{IiG}	$128.1 + 37.6log_{10}(d_{IiG})$ [32]
PL_{GD}	$148 + 40log_{10}(d_{GD})$ [32]
PL_{DjD}	$148 + 40log_{10}(d_{DjD})$ [32]

Figure 13 depicts the effect of the interfering transmission power on the overall system energy efficiency (EE). Five different scenarios have been assumed to determine the effect of the interfering devices' transmission power on the system performance. Figure 13a shows the effect of the interfering devices' transmission power when the transmission distance between the smart monitoring device and the gateway (d_{SG}) is 50 m and the transmission distance between the gateway and the medical reception (d_{GD}) is 50 m. Under this condition, it can be found that decreasing the interfering device transmission leads to a decrease in the system energy efficiency, and then, increases the system losses which leads to inefficiently receiving the information. Additionally, it can be mentioned from Figure 13b that when assuming that d_{SG} is 100 m and d_{GD} is 100 m the maximum EE can be achieved when the interfering device transmission power is 3 dBm either the received message will be lost or will be received with bad quality. Furthermore, when assuming that d_{SG} is 150 m or 200 m and d_{GD} is 150 m or 200 m as shown in Figure 13c,d the maximum EE can be reached when the interfering device transmission power is 11 dBm. Moreover, when d_{SG} is 250 m and d_{GD} is 250 m the required interfering device transmission power to reach the maximum EE will be 13 dBm. It can be concluded from this figure that decreasing the distance between any source and destination for reaching the maximum EE and ensuring

that the system is reliably required decreases the interfering device transmission, this can be obtained by trying to disable any transmission devices existing in the same area o the smart monitor device or keeping the smart monitor devices far way from any interfering devices. Additionally, it can be mentioned that when the interfering device transmission power increases the required transmission power for the smart monitor and the gateway must increase to overcome the effect of the interference and at the same time reach the required system QoS.

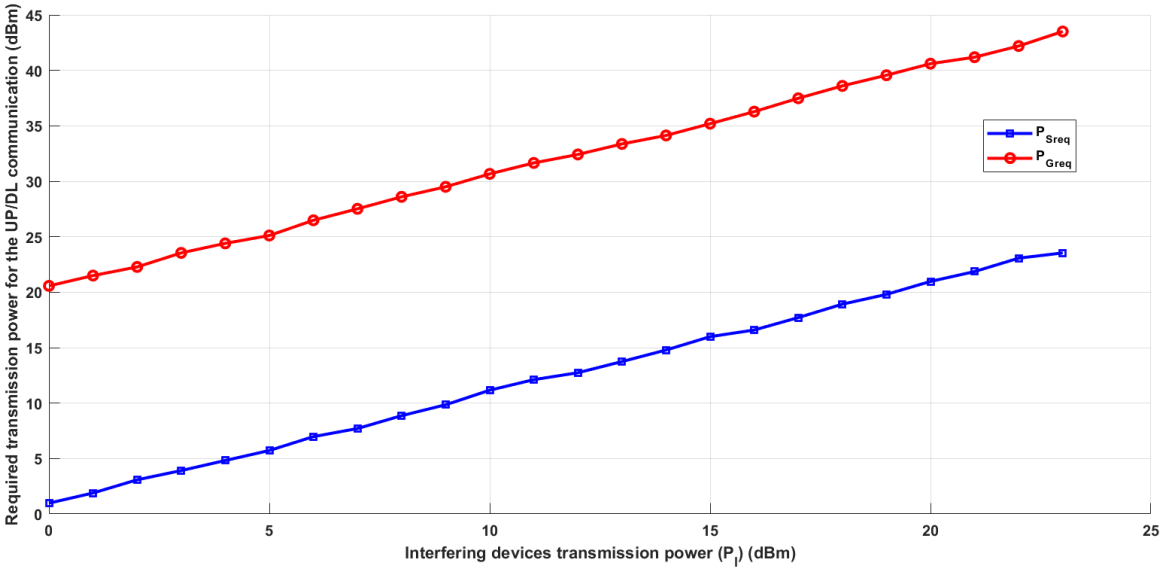

Figure 12. Required transmission power for the UP/DL communication (dBm) versus interfering devices' transmission power (P_I) (dBm).

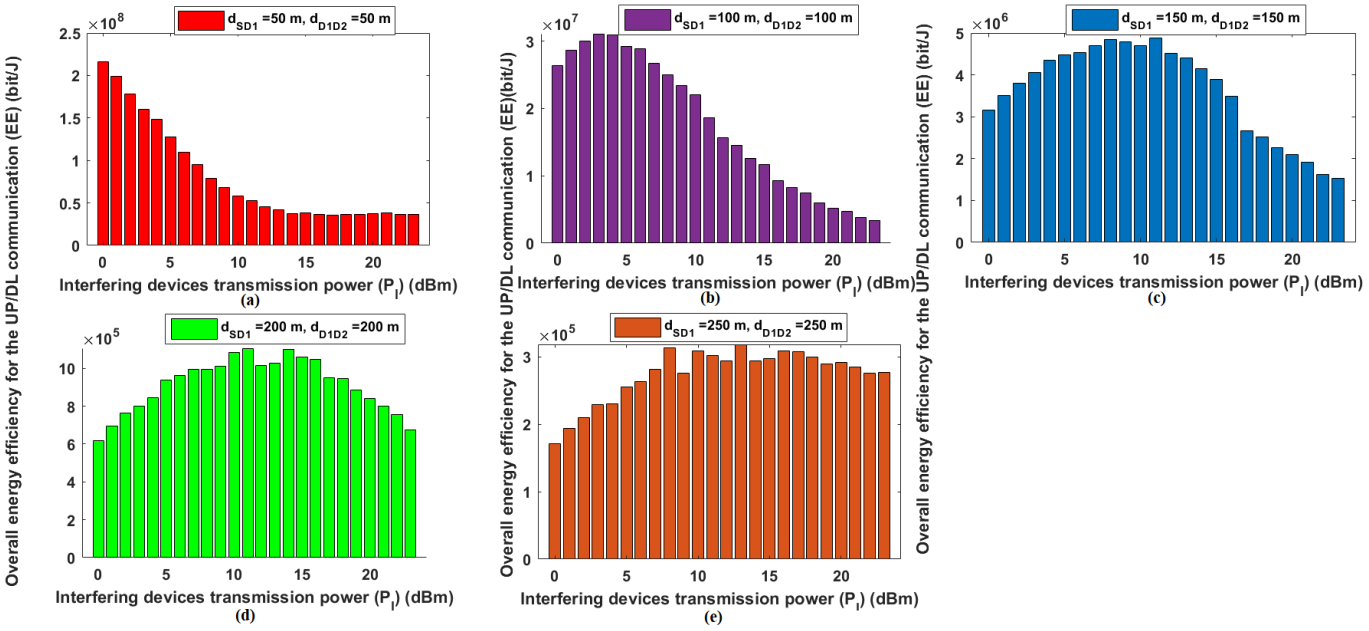

Figure 13. Overall energy efficiency for the UP/DL communication (EE) (bit/J) versus interfering devices' transmission power (P_I) (dBm). Subfigures (**a**–**e**) correspond to distances between source S1 and destination D1 and between destinations D1 and D2 of 50 m, 100 m, 150 m, 200 m, and 250 m, respectively.

Figure 14 demonstrates the required smart monitor devices and gateway transmission power to reach the required system QoS. Figure 14a,b show that for the uplink and downlink

transmission when the required QoS increases, the transmission power for both smart monitor devices and gateway must increase to satisfy the required QoS. Moreover, it can be noted when comparing Figure 14a,b that the required gateway transmission power is always greater than the required smart monitor device transmission power, whether the interfering transmission device is 17 dBm or 23 dBm, this is because the gateway is always facing interference greater than any other receiving device as the gateway is considered the main source that can easily communicate with all its surrounding devices and coordinate the communication among them.

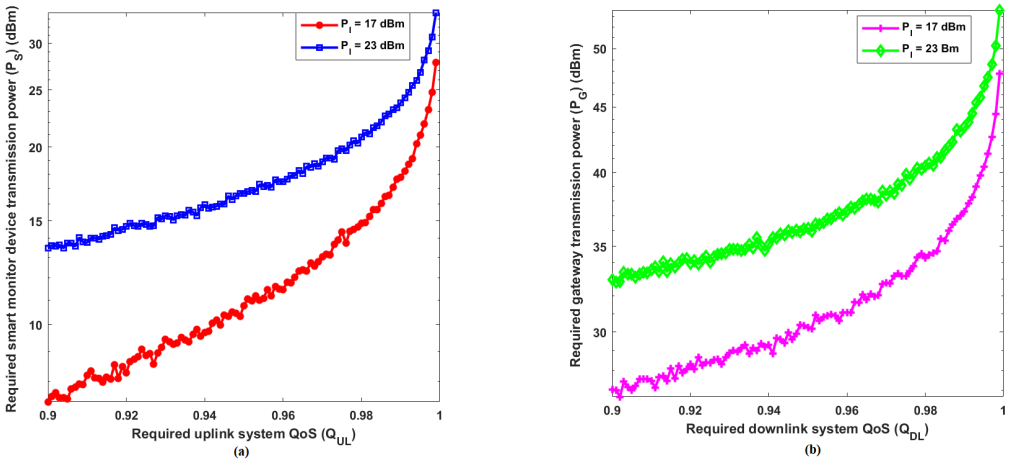

Figure 14. (**a**) Required smart monitor device transmission power (P_{Sreq}) (dBm) versus the required uplink QoS (Q_{UL}). (**b**) Required gateway transmission power (P_{Sreq}) (dBm) versus the required downlink QoS (Q_{DL}).

5. Discussion

This study presents a comprehensive framework for minimizing the MMR by addressing both region-level and patient-level factors. The proposed framework proposes an XAI-enabled deep learning model to identify high-risk regions and patients, which can then lead to early healthcare intervention. Furthermore, the presented framework ensures efficient and secure data transmission between patients and healthcare centers.

The region-level analysis demonstrated the effectiveness of the proposed XAI-based model in identifying regions with high MMR risk. The model accurately classified regions based on various factors such as demographics, healthcare access, and maternal health indicators. The SHAP analysis provided valuable elaboration into the key factors driving the model's predictions, allowing healthcare personnel to target interventions effectively.

The patient-level analysis presented the potential of the proposed XAI-based model to identify high-risk patients. The model accurately classified patients based on physiological parameters and demographic information. The LIME analysis provided interpretable explanations for the model's predictions, enabling healthcare providers to understand the underlying reasons for a patient's risk assessment.

The proposed IoMT framework ensures efficient and secure data transmission from patient devices to healthcare providers. The energy-efficient transmission scheme optimizes resource utilization, while the robust security measures safeguard patient privacy and data integrity.

While the proposed framework shows promising results, future research needs to address some limitations. One limitation is the reliance on accurate and reliable data. Data quality and completeness can significantly impact the performance of the models. Another limitation is the generalizability of the models to different regions and healthcare settings. Further research is needed to evaluate the performance of the models in diverse contexts. Several future directions could result from this work, such as integrating more data, developing more sophisticated models, and exploring missing data.

6. Conclusions

In this article, the MMR problem was addressed by building a model that has a global perspective and monitors it at the region and patient levels. The region-based assessment evaluated each region, and accordingly, the risk level was calculated. The second area of focus was providing continuous vital signs monitoring for expectant women in high-risk areas to issue alerts for medium- and high-risk instances. The patient's medical records at the data center and the hospital contain a record of this alert, which is efficiently and securely delivered through an efficient communication system, and then, recorded to allow for future intervention. It became crucial to select an explainable model that would offer an analytical evaluation of the outcomes because the themes treated are extremely sensitive both at the national and patient levels. To assess the trade-off between model performance and interpretability, this study analyzed high-performance deep learning with explainable models. The results demonstrated that the proposed CNN-GRU model achieved superior performance to state-of-the-art benchmarks and other published research while offering explainable outcomes. The performance of both systems was evaluated by analyzing the importance of key features, identifying feature relationships, and examining the underlying methodology used to determine risk. This analysis allowed for a comprehensive understanding of how each model arrived at its predictions. The explainability of the chosen model will enhance its usage among medical staff. As for future work, more data will be collected to include further details of each patient and to which region they belong. Accordingly, a deeper level of interpretation could be included to link the state-level and patient-level risks. This will help in gaining a better understanding of the risk variations within different regions.

Author Contributions: Conceptualization: S.N.S.; data curation: S.N.S. and R.A.O.; formal analysis: S.N.S., R.A.O. and Y.N.M.S.; investigation: S.N.S. and R.A.O.; methodology: S.N.S. and R.A.O.; resources: S.N.S., R.A.O., Y.N.M.S. and M.N.E.; software: S.N.S. and R.A.O.; validation: S.N.S. and R.A.O.; visualization: S.N.S. and R.A.O.; resources: S.N.S., R.A.O., Y.N.M.S. and M.N.E.; writing—review and editing, S.N.S., R.A.O., Y.N.M.S., and M.N.E. All authors have read and agreed to the published version of the manuscript.

Funding: This research received no external funding.

Data Availability Statement: The data that supports the findings of this study are available from https://www.kaggle.com/datasets/csafrit2/maternal-health-risk-data accessed on 9 October 2024 and from https://www.kaggle.com/datasets/sourabhshastri/maternal-health-dataset accessed on 9 October 2024.

Conflicts of Interest: The authors declare no conflicts of interest.

References

1. WHO. Maternal Mortality. 2024. Available online: https://www.who.int/news-room/fact-sheets/detail/maternal-mortality (accessed on 30 September 2024)
2. Khadidos, A.O.; Saleem, F.; Selvarajan, S.; Ullah, Z.; Khadidos, A.O. Ensemble machine learning framework for predicting maternal health risk during pregnancy. *Sci. Rep.* **2024**, *14*, 21483. [CrossRef] [PubMed]
3. Yin, Y.; Bingi, Y. Using machine learning to classify human fetal health and analyze feature importance. *BioMedInformatics* **2023**, *3*, 280–298. [CrossRef]
4. Silva Rocha, E.d.; de Morais Melo, F.L.; de Mello, M.E.F.; Figueiroa, B.; Sampaio, V.; Endo, P.T. On usage of artificial intelligence for predicting mortality during and post-pregnancy: A systematic review of literature. *BMC Med. Inform. Decis. Mak.* **2022**, *22*, 334. [CrossRef]
5. Loh, H.W.; Ooi, C.P.; Seoni, S.; Barua, P.D.; Molinari, F.; Acharya, U.R. Application of Explainable Artificial Intelligence for Healthcare: A Systematic Review of the Last Decade (2011–2022). *Comput. Methods Programs Biomed.* **2022**, *226*, 107161. Available online: https://dl.acm.org/doi/10.1016/j.cmpb.2022.107161 (accessed on 9 October 2024).
6. Islam, M.N.; Mustafina, S.N.; Mahmud, T.; Khan, N.I. Machine learning to predict pregnancy outcomes: A systematic review, synthesizing framework and future research agenda. *BMC Pregnancy Childbirth* **2022**, *22*, 348. [CrossRef]
7. Dawodi, M.; Wada, T.; Baktash, J.A. Applicability of ICT, Data Mining and Machine Learning to Reduce Maternal Mortality and Morbidity: Case Study Afghanistan. *Int. Inf. Inst. Inf.* **2020**, *23*, 33–45.

8. Ahmed, M.; Kashem, M.A.; Rahman, M.; Khatun, S. Review and analysis of risk factor of maternal health in remote area using the Internet of Things (IoT). In Proceedings of the InECCE2019, Kuantan, Malaysia, 29 July 2019; pp. 357–365.
9. Ahmed, M.; Kashem, M.A. IoT based risk level prediction model for maternal health care in the context of Bangladesh. In Proceedings of the 2020 2nd International Conference on Sustainable Technologies for Industry 4.0 (STI), Dhaka, Bangladesh, 19–20 December 2020; IEEE: Piscataway, NJ, USA, 2020; pp. 1–6.
10. Alam, M.S.B.; Patwary, M.J.; Hassan, M. Birth mode prediction using bagging ensemble classifier: A case study of bangladesh. In Proceedings of the 2021 International Conference on Information and Communication Technology for Sustainable Development (ICICT4SD), Dhaka, Bangladesh, 27–28 February 2021; IEEE: Piscataway, NJ, USA, 2021; pp. 95–99.
11. Shastri, S.; Kour, P.; Kumar, S.; Singh, K.; Sharma, A.; Mansotra, V. A nested stacking ensemble model for predicting districts with high and low maternal mortality ratio (MMR) in India. *Int. J. Inf. Technol.* **2021**, *13*, 433–446. [CrossRef]
12. Adedinsewo, D.A.; Johnson, P.W.; Douglass, E.J.; Attia, I.Z.; Phillips, S.D.; Goswami, R.M.; Yamani, M.H.; Connolly, H.M.; Rose, C.H.; Sharpe, E.E.; et al. Detecting cardiomyopathies in pregnancy and the postpartum period with an electrocardiogram-based deep learning model. *Eur. Heart J.-Digit. Health* **2021**, *2*, 586–596. [CrossRef]
13. Patel, S.S. Explainable machine learning models to analyse maternal health. *Data Knowl. Eng.* **2023**, *146*, 102198. [CrossRef]
14. Ramakrishnan, R.; Rao, S.; He, J.R. Perinatal health predictors using artificial intelligence: A review. *Women's Health* **2021**, *17*, 17455065211046132. [CrossRef]
15. Yang, G.; Ye, Q.; Xia, J. Unbox the black-box for the medical explainable AI via multi-modal and multi-centre data fusion: A mini-review, two showcases and beyond. *Inf. Fusion* **2022**, *77*, 29–52. [CrossRef]
16. Nti, I.K.; Owusu-Boadu, B. A hybrid boosting ensemble model for predicting maternal mortality and sustaining reproductive. *Smart Health* **2022**, *26*, 100325. [CrossRef]
17. Bogale, D.S.; Abuhay, T.M.; Dejene, B.E. Predicting perinatal mortality based on maternal health status and health insurance service using homogeneous ensemble machine learning methods. *BMC Med. Inform. Decis. Mak.* **2022**, *22*, 341. [CrossRef]
18. Hireche, R.; Mansouri, H.; Pathan, A.S.K. Security and Privacy Management in Internet of Medical Things (IoMT): A Synthesis. *J. Cybersecur. Priv.* **2022**, *2*, 640–661. [CrossRef]
19. Osman, R.A.; Saleh, S.N.; Saleh, Y.N.; Elagamy, M.N. A Reliable and Efficient Tracking System Based on Deep Learning for Monitoring the Spread of COVID-19 in Closed Areas. *Int. J. Environ. Res. Public Health* **2021**, *18*, 12941. [CrossRef]
20. Hatzivasilis, G.; Soultatos, O.; Ioannidis, S.; Verikoukis, C.; Demetriou, G.; Tsatsoulis, C. Review of security and privacy for the Internet of Medical Things (IoMT). In Proceedings of the 2019 15th international conference on distributed computing in sensor systems (DCOSS), Santorini Island, Greece, 29–31 May 2019; IEEE: Piscataway, NJ, USA, 2019; pp. 457–464.
21. Adil, M.; Khan, M.K.; Kumar, N.; Attique, M.; Farouk, A.; Guizani, M.; Jin, Z. Healthcare Internet of Things: Security Threats, Challenges and Future Research Directions. *IEEE Internet Things J.* **2024**, *11*, 19046–19069. [CrossRef]
22. Raeisi-Varzaneh, M.; Dakkak, O.; Alaidaros, H.; Avci, İ. Internet of Things: Security, Issues, Threats, and Assessment of Different Cryptographic Technologies. *J. Commun.* **2024**, *19*, 78–89. [CrossRef]
23. Garg, N.; Wazid, M.; Singh, J.; Singh, D.P.; Das, A.K. Security in IoMT-driven smart healthcare: A comprehensive review and open challenges. *Secur. Priv.* **2022**, *5*, e235. [CrossRef]
24. Shahid, J.; Ahmad, R.; Kiani, A.K.; Ahmad, T.; Saeed, S.; Almuhaideb, A.M. Data protection and privacy of the internet of healthcare things (IoHTs). *Appl. Sci.* **2022**, *12*, 1927. [CrossRef]
25. Zhang, Q.; Zhang, L.; Liang, Y.C.; Kam, P.Y. Backscatter-NOMA: A symbiotic system of cellular and Internet-of-Things networks. *IEEE Access* **2019**, *7*, 20000–20013. [CrossRef]
26. ElHalawany, B.M.; Ruby, R.; Wu, K. D2D communication for enabling Internet-of-Things: Outage probability analysis. *IEEE Trans. Veh. Technol.* **2019**, *68*, 2332–2345. [CrossRef]
27. Chettri, L.; Bera, R. A comprehensive survey on Internet of Things (IoT) toward 5G wireless systems. *IEEE Internet Things J.* **2019**, *7*, 16–32. [CrossRef]
28. Siddiqui, M.U.A.; Qamar, F.; Ahmed, F.; Nguyen, Q.N.; Hassan, R. Interference management in 5G and beyond network: Requirements, challenges and future directions. *IEEE Access* **2021**, *9*, 68932–68965. [CrossRef]
29. Li, X.; Ma, L.; Shankaran, R.; Xu, Y.; Orgun, M.A. Joint power control and resource allocation mode selection for safety-related V2X communication. *IEEE Trans. Veh. Technol.* **2019**, *68*, 7970–7986. [CrossRef]
30. Choi, J.Y.; Jo, H.S.; Mun, C.; Yook, J.G. Deep reinforcement learning-based distributed congestion control in cellular V2X networks. *IEEE Wirel. Commun. Lett.* **2021**, *10*, 2582–2586. [CrossRef]
31. Huang, Y.; Liu, M.; Liu, Y. Energy-efficient SWIPT in IoT distributed antenna systems. *IEEE Internet Things J.* **2018**, *5*, 2646–2656. [CrossRef]
32. Liu, Z.; Chan, K.Y.; Ma, K.; Guan, X. Chance-constrained optimization in D2D-based vehicular communication network. *IEEE Trans. Veh. Technol.* **2019**, *68*, 5045–5058. [CrossRef]

Disclaimer/Publisher's Note: The statements, opinions and data contained in all publications are solely those of the individual author(s) and contributor(s) and not of MDPI and/or the editor(s). MDPI and/or the editor(s) disclaim responsibility for any injury to people or property resulting from any ideas, methods, instructions or products referred to in the content.